Muhammad Farhan | Deeptangshu Chaudhary | Ulrich Nöchel | Marc Behl | Karl Kratz | Andreas Lendlein

Electrical actuation of coated and composite fibers based on poly[ethylene-co-(vinyl acetate)]

Suggested citation referring to the original publication:
Macromolecular materials and engineering 306 (2020) 2, Art. 2000579
DOI https://doi.org/10.1002/mame.202000579
ISSN 1438-7492, 1439-2054

Journal article | Version of record

Secondary publication archived on the Publication Server of the University of Potsdam:
Zweitveröffentlichungen der Universität Potsdam : Mathematisch-Naturwissenschaftliche Reihe 1375
ISSN: 1866-8372
https://nbn-resolving.org/urn:nbn:de:kobv:517-opus4-571679
DOI: https://doi.org/10.25932/publishup-57167

Macromolecular Materials and Engineering
www.mme-journal.de

Electrical Actuation of Coated and Composite Fibers Based on Poly[ethylene-*co*-(vinyl acetate)]

*Muhammad Farhan, Deeptangshu Chaudhary, Ulrich Nöchel, Marc Behl, Karl Kratz, and Andreas Lendlein**

Robots are typically controlled by electrical signals. Resistive heating is an option to electrically trigger actuation in thermosensitive polymer systems. In this study electrically triggerable poly[ethylene-*co*-(vinyl acetate)] (PEVA)-based fiber actuators are realized as composite fibers as well as polymer fibers with conductive coatings. In the coated fibers, the core consists of crosslinked PEVA (cPEVA), while the conductive coating shell is achieved via a dip coating procedure with a coating thickness between 10 and 140 μm. The conductivity of coated fibers σ = 300–550 S m^{-1} is much higher than that of the composite fibers σ = 5.5 S m^{-1}. A voltage (*U*) of 110 V is required to heat 30 cm of coated fiber to a targeted temperature of ≈ 65 °C for switching in less than a minute. Cyclic electrical actuation investigations reveal ε'_{rev} = 5 ± 1% reversible change in length for coated fibers. The fabrication of such electro-conductive polymeric actuators is suitable for upscaling so that their application potential as artificial muscles can be explored in future studies.

1. Introduction

Electrically driven soft actuators are highly desirable for future robotic applications. Shape-memory polymer actuators are capable of defined, programmable thermoreversible movements and have emerged as promising candidate materials for applications, where regulated as well as adaptive movement is required.[1–4] These actuating materials can be used in different forms such as 3D bulky objects, 2D films, or as fibers. Among these, the fibrous actuators have attracted attention, as they provide flexibility and high anisotropic properties and are capable of very complex actuation behavior.[5,6] Tensile and torsional actuations can be realized in fibers when subjected to a constant external stress, while fibers also need to be programmed by twisting or coiling in a post manufacturing process.[7–9] Free-standing reversible actuators are required for applications, where a reversible muscle-like movement should be realized – by only a single actuator. As shape-memory polymer actuators[10] or shape-memory composite fibers[11] are typically thermally controlled, their applicability in robotic applications would benefit, if they could be electrically actuated. Here we aim at shape-memory polymer fibers, which are electrically actuable and could be scaled-up in a conventional manufacturing environment.

Resistive heating or Joule heating, as popularly known, can be achieved in conductive polymeric systems, which is due to their resistance to the flow of current. Conductive composites as well as conductive coatings can be developed to realize joule/resistive heating in polymers.[12–14] Metal particles, carbon-based inorganic conductive fillers or conductive polymers are used to achieve conductivity in polymeric materials for joule heating.[15–17] Heating phenomena in composites rely on incorporation of a conductive filler in the core enabling heat generation inside the core material and heat transfer to the polymer matrix. In the coating approach, the conductive material forms a shell on the fiber surface. When a certain voltage is applied, heat is generated at the surface and is transferred to the fiber core. In addition to the physical principles, some engineering principles also need to be considered. Incorporation of inorganic fillers lead to disturbance of crystallites in the polymer matrix and affect other properties related to these crystallites, such as shape-memory properties. A filler content up to 40 wt% is reported in shape-memory polymer composites.[18,19] Similarly, a coating might add stiffness to fibers, which could lead to hinder the movement of core material.

In this study, we present electrically triggered fiber actuators to overcome the limitations of thermally driven actuators by transferring actuator technology to polymeric fibers and enabling joule heating to trigger actuation function at the same time. We aimed at an actuation, which can be triggered by resistive heating within a domestic voltage supply range. Our concept was to use carbon-based conductive fillers such as carbon black (CB), carbon nanotubes (CNTs) and graphene

Dr. M. Farhan, Dr. D. Chaudhary, Dr. U. Nöchel, Dr. M. Behl, Dr. K. Kratz, Prof. A. Lendlein
Institute of Biomaterial Science and Berlin-Brandenburg Center for Regenerative Therapies
Helmholtz-Zentrum Geesthacht
Kantstr. 55, 14513 Teltow, Germany
E-mail: andreas.lendlein@hzg.de
Prof. A. Lendlein
Institute of Chemistry
University of Potsdam
Karl-Liebknecht-Str. 24–25, 14476 Potsdam, Germany
The ORCID identification number(s) for the author(s) of this article can be found under https://doi.org/10.1002/mame.202000579.

DOI: 10.1002/mame.202000579

nano-platelets to prepare composite as well as coated conductive fibers based on poly[ethylene-*co*-(vinyl acetate)] (PEVA). Among the polymer systems capable of actuation like copolymer networks from poly(ε-caprolactone) and poly(ω-pentadecalactone) or AB networks from poly(ε-caprolactone) and butyl acrylate as well as crosslinked PEVA films, only the PEVA based systems provides a broad actuation temperature range spanning over several 10 K.[4] Furthermore, the PEVA based system enables processing by extrusion as the crosslinking of the PEVA can be achieved in a post processing step.[20] In this previously reported post processing procedure for torsional fiber actuators PEVA was mixed with a crosslinker in melt, cured and subsequently programmed by deformation. The hypothesis of our work was that alternatively the molecular chain orientation required for reversible fiber actuation could be achieved by shear-induced orientation during shaping via melt extrusion for stretching and contraction. Therefore, PEVA was selected as matrix material for the actuating fibers. The fibers can be crosslinked by gamma beam irradiation at ambient temperature to preserve the crystallite orientation achieved during extrusion. Reversible actuation in such materials is related to entropic recovery or melting induced contraction (MIC) of oriented crystallites on heating by resistive heating and crystallization induced elongation (CIE) on cooling. The challenge for composite fiber engineering was to achieve an optimal balance among filler content and conductivity without negatively influencing actuation properties and vice versa. As it was anticipated that crosslinking should not influence the conductivity, at first non-crosslinked composite fibers were investigated and if these meet the demands of the necessary conductivity for Joule heating, then the actuation capability of crosslinked composite fibers should be investigated. For the coated fibers, our strategy was to achieve sufficient elasticity of the coating layer to allow expansion and contraction of the fiber core during reversible actuation, where conductivity is not affected by the actuation. Furthermore, adhesion of coating to the fiber core was important and delamination of coating during reversible actuation must be avoided for a reliable multi-cyclic actuation.

2. Results and Discussion

In CB-based composite fibers, the weight content of CB was varied between 5 and 50 wt%, however these fibers did not show any conductivity. Similarly, fibers with 2.5 and 5 wt% graphene were non-conductive. Fibers with 20 wt% CB and 10 wt% graphene (PEVA20CB10G) on the other hand were conductive with poor conductivity (σ) 5.5 S m^{-1} and higher resistivity (ρ) 0.19 Ω m. Carbon black particles must be connected to each other to create a conductive channel in order to have conductivity as schematically illustrated in **Figure 1**, which might not be possible with a CB concentration of ≤50 wt%. As further increase in filler content could effect crystallites and related shape-changing properties, filler concentrations above 50 wt% were not prepared.[18] In PEVA20CB10G, graphene nano-platelets might act as a bridge between the CB particles to create a conductive channel and this would result in conductive fibers.[21]

Conductivity of coated fibers was compared with composite fibers. Conductive coatings were prepared using CB, CNTs and graphene. Details of the coating formulations can be found in Table S1 (Supporting Information). PEVA was used to provide adhesion to core fiber's surface and to enhance flexibility of the coatings, however lower concentration ≈1 wt% of PEVA was used to minimize its effect on the conductivity. Core (actuating) fibers were prepared from PEVA and irradiated by gamma beam in the second step to achieve crosslinking. Generally, coated fibers had a higher conductivity and lower resistivity compared to the composite fibers. However, coating layers from CNTs-based coating were very non-uniform with low $\sigma \approx 99$ S m^{-1} and were not further investigated, see coating images in Figure S1 (Supporting Information). On the other hand, graphene-based coating was too stiff to allow any movement of the fiber for reversible actuation, therefore it was excluded too. In contrast, fibers coated with CB-based coating had a uniform coating thickness and better elasticity. The conductivity of the fibers coated with a solution containing a 1:1 ratio of PEVA to CB was ≈415 S m^{-1}, while resistivity was around 0.00241 Ω m. Higher conductivity of coated fibers can be attributed to higher filler content to polymer ratio as compared to composite fibers.

A textile prepared from CB-based coated conductive fibers demonstrates a proof of the concept of electrically triggered actuation and wool fibers as shown in Figure 1C. Black conductive fibers were used as warp (in length), while white colored wool fibers were inserted as weft (in width) to prepare a textile actuator. Infrared (IR) images presented in Figure 1D show that heating can be achieved by applying voltage, which triggers the actuation of fibers leading to folding and unfolding of this textile reversibly as shown in the images in Figure 1E and in Video S1 (Supporting Information). Therefore, heating of composite and coated fibers was investigated in detail and the results are shown in **Figure 2**A. Voltage was applied to the fibers and surface temperature was recorded by IR camera for a fixed fiber length of 30 cm. An increase in voltage led to a higher temperature in both fiber types; however, the temperature for coated fibers was much higher than the composite fiber with similar applied voltages. For the coated fiber cPEVA-CB2 heating starts at a lower applied voltage of 30 V and a temperature of ≈65 °C could be achieved with 110 V. A further increase in voltage to 140 V raised the temperature to ≈85 °C. However, a maximum observed temperature for the composite fiber PEVA20CB10G was ≈45 °C with a comparatively higher voltage of 200 V. Furthermore, heating of PEVA20CB10G was not uniform and temperature on some sections was higher than on the rest of the fiber. This could be due to inhomogeneous filler distribution in the composite fibers. An increase in voltage to 250 V led to burning at these higher temperature spots and breaking of the fiber. In contrast, heating of coated fibers was uniform along the full fiber length. Both fiber types could be successfully heated, whereas higher temperatures in cPEVA-CB2 can be attributed to a higher conductivity and lower resistivity of coated fibers compared to PEVA20CB10G. Change in current for the voltage applied is shown in Figure S2 (Supporting Information) for both fibers.

Furthermore, the influence of filler distribution within the polymer matrix in composite fibers or in coating on conductivity and relative joule heating was explored. Scanning electron microscopy (SEM) images of composite fibers showed a homogeneous distribution of CB in the polymer matrix as

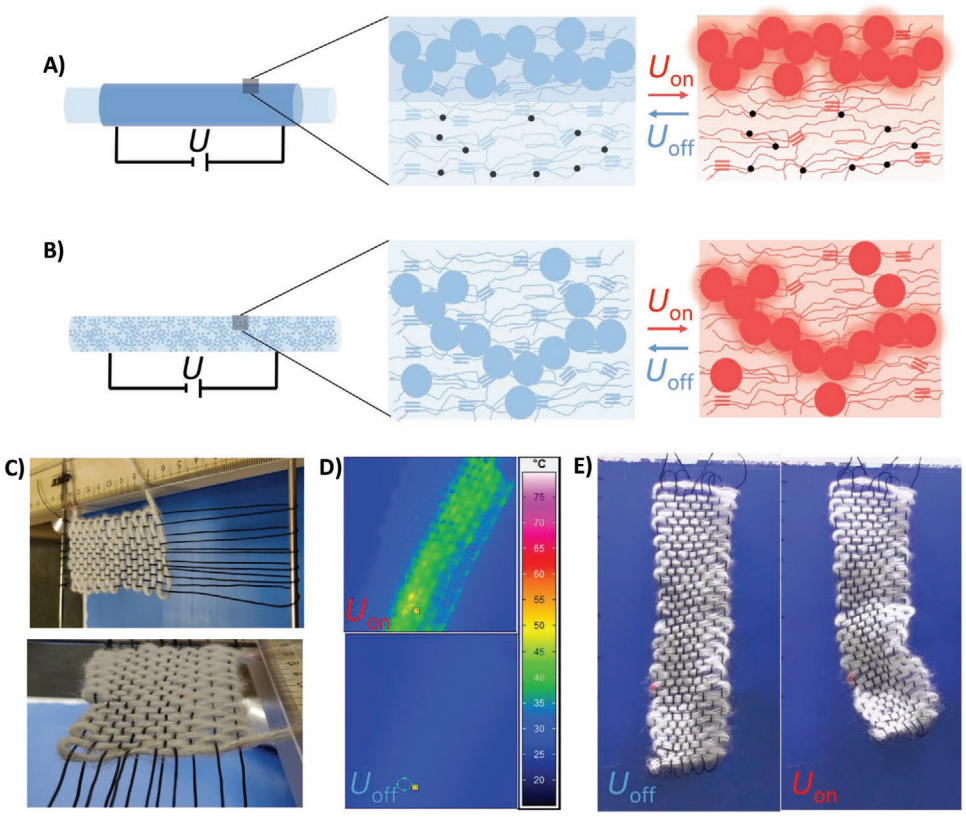

Figure 1. Schematic illustration of joule heating in coated and composite fibers. A) In the coated fiber, heating takes place in the conductive coating shell (at fiber surface) and heat then transfers to the actuating fiber core. B) In composite fibers, heating is achieved by the embedded conductive materials in the fiber core and heat transfer to the polymer matrix. The molecular mechanism in the course of joule heating with voltage OFF is presented with (〓) PE crystals, (●) covalent netpoints, (●) inorganic conductive filler (carbon black) and (∿) amorphous polymer segments, while with voltage ON is presented with (〓) PE crystals, (●) covalent netpoints, (●) inorganic conductive filler (carbon black) and (∿) amorphous polymer segment indicating heating of polymer matrix by joule heating from conductive filler. C) A textile construct from coated conductive fibers (in warp) and wool (in weft). D) IR images of this textile with voltage ON and OFF. E) Reversible actuation by switching the voltage source ON and OFF reversibly.

presented in Figure S3 (Supporting Information). However, in PEVA20CB10G, some aggregates of graphene nano-platelets and CB were observed, see Figure 2B-iii,iv. This aggregation of conductive fillers might be a reason for the inhomogeneous heating observed in the composite fibers, which led to burning and breaking of the fibers at these sections. Similarly, coating thickness and morphology in coated fibers was analyzed. To achieve a coating layer with a thickness higher than 10 µm, the concentration of CB in the coating solution was increased. Figure S3B (Supporting Information) shows that a

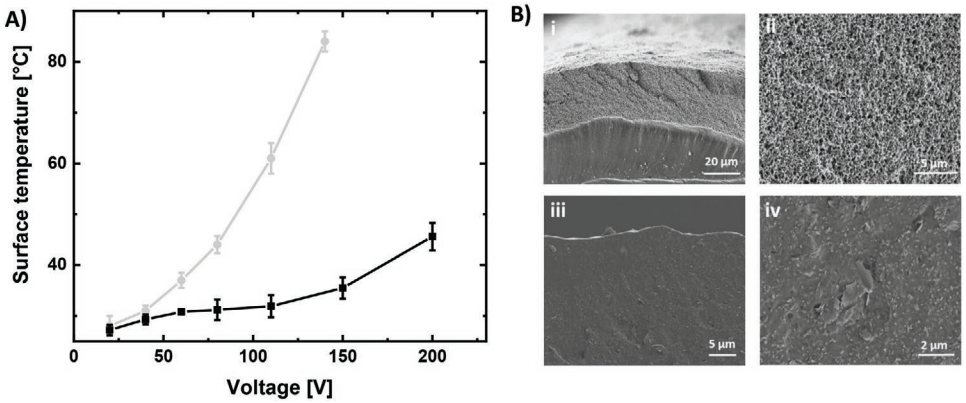

Figure 2. A) Surface temperature of the fiber due to joule heating by applied voltage for coated fiber cPEVA-CB2 (grey circle and line) and for composite fiber PEVA20CB10G (black line and square). The data is representative of five samples (mean ± standard deviation). B) SEM images of cross-sections of cPEVA-CB2 (i,ii) and of PEVA20CB10G (iii,iv).

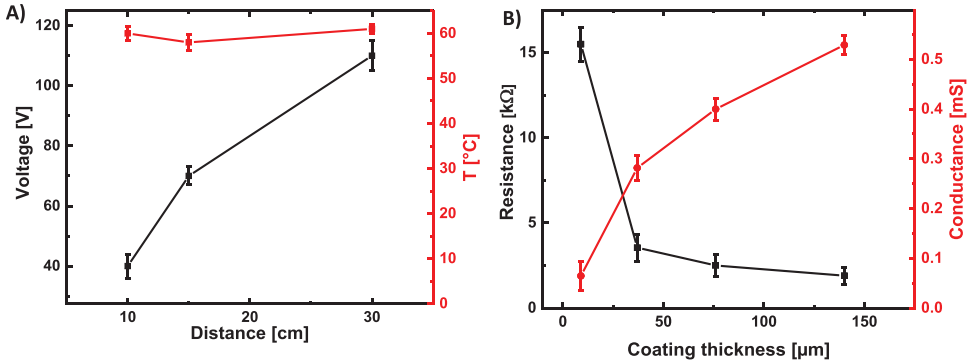

Figure 3. A) Changes in the required voltage (with change in fiber length) to reach the required temperature for coated fiber cPEVA-CB2. B) Change in the resistance and conductance of the coated fibers with change in coating thickness over 10 cm fiber length. The data is representative of five samples (mean ± standard deviation).

coating solution with a higher CB content resulted in increased coating thickness. This thickness could reach to 140 µm with the same dipping procedure with a formulation containing 4 g of CB. However, higher thickness (or higher CB to polymer ratio) resulted in poor adhesion of the coating to the fiber core and a delamination of the coating layer was observed in some cases. The images presented in Figure 2B-i,ii show the porous coating layers with a thickness of 37 µm for cPEVA-CB2. Porosity can increase resistivity and reduce conductivity, consequently effecting the joule heating capability. This porosity can be attributed to fast evaporation of the solvent (toluene) in the coating solution. Solvents such as xylene, THF, DMF and DMSO were also tried to eliminate/reduce porosity, but those coating were porous, too. In addition, not all solvents created stable and homogeneous emulsions, and coating with sufficient layer thicknesses were not achievable. Interestingly, a coating formulation with a 1:1 ratio of CB and PEVA resulted in a non-porous coating layer of thickness ≈10 µm as shown in Figure S3B-i,ii (Supporting Information). In this sponge like porous coating morphology, CB particles seemed connected to form a conductive channel, which was difficult to observe in the composite fiber, which consequently resulted in a large difference in σ and ρ of both conductive fibers.

Joule heating is related to the resistance and to the current flowing through a conductive material. To investigate this, coating thickness and fiber length on resistance/conductance as well as joule heating were analyzed. Fiber length was varied as 10, 15, and 30 cm while surface temperature was measured for a specific applied voltage. The required voltage to achieve a stable surface temperature of ≈65 °C for different fiber lengths is shown in **Figure 3**A for cPEVA-CB2. A fiber length of 10 cm required 40 ± 3 V to reach to ≈65 °C, while the required voltage increased to 110 ± 5 V for a length of 30 cm. Relative current values for aforementioned fiber lengths are presented in Figure S4 (Supporting Information) where a current of around 20 mA was recorded. The results for PEVA20CB10G are presented in Figure S5 (Supporting Information), where a similar trend can be seen. A temperature ≈65 °C for 30 cm composite fiber could not be achieved due to high resistivity of composite fibers. The change in voltage to achieve similar joule heating effect for various fiber lengths is due to a change in the fiber conductance. The conductance and consequently the heating capability was lower if electrodes were further apart, meaning a longer fiber length, therefore higher voltages were required to achieve similar current values and heating effect.

Similarly, the effect of coating thickness on conductance and resistance was analyzed. The changes in conductance and resistance of the fibers for a fixed length of 10 cm are presented in Figure 3B. The highest resistance of 15.5 ± 1 kΩ was observed for cPEVA-CB1 fibers with a lower coating thickness of 10 µm, where conductance was around 0.065 mS. A drastic decrease in resistance to 3.5 ± 0.7 kΩ was observed for cPEVA-CB2 for the same length as coating thickness increased from 10 to 37 µm for this fiber sample. Further increase in coating thickness also showed a decrease in resistance but this change was not significant. A reciprocal trend for conductance can be seen from Figure 3B. Required voltage for these fibers to achieve a temperature around 65 °C is presented in Figure S6 (Supporting Information). Based on adhesion and resistance analysis, which is related to coating thickness, fibers with a coating thickness ≤40 µm were considered more suitable for actuation purpose. The relative analysis for composite fibers was not possible, as the fiber diameter was not varied. The effect of geometry on joule heating helped to define the voltage range for different fiber lengths, which later is used for actuation investigation of these fibers.

The effect of fillers on thermal as well as mechanical properties was investigated, and the results were compared with that of bulk PEVA material. These investigations are relevant for actuation investigation as they help to define parameters for those investigations. Thermal properties were also investigated and a broad melting transition from 40 to 80 °C related to the crystalline PE domains was observed for all coated and composite fibers with a melting peak at T_m = 66 ± 2 °C and crystallization peak at T_c = 43 ± 2 °C. A slightly higher T_m = 71 ± 1 °C and T_c = 50 ± 1 °C was observed for CB-based composite fibers, which was comparable to the starting polymer PEVA. The lower T_m of coated fibers can be attributed to the crosslinking of the core PEVA fiber, which affects crystallization and consequently results in lowering the T_m peak. Tensile tests at ambient temperature revealed a Young's modulus E = 33 ± 2 MPa for cPEVA core fibers with elongation at break ε_b = 405 ± 40%. Coated fibers showed similar results, however a higher E = 57 ± 2 MPa and lower ε_b = 325 ± 21% was noticed for the

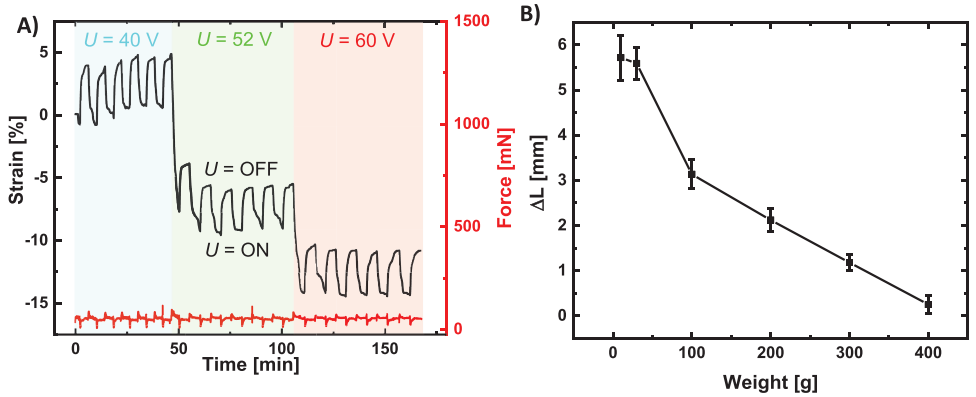

Figure 4. A) Cyclic change in strain for cPEVA-CB2 in stress-free electrical actuation experiments by switching voltage source ON and OFF. B) Change in length during electrical actuation of the fiber as a function of applied weight for coated fiber cPEVA-CB1. The mean and standard deviation in reversible actuation were calculated from the changes in the different cycles within one cyclic test.

PEVA20CB10G composite fiber. Interestingly, E for CB-based coated fibers was between 24 and 30 MPa with ε_b in range of 550% and 1030%. The results are listed in Table S2 (Supporting Information) for all fibers.

A detailed analysis of conductance, resistance and joule heating helped to identify the voltage range required for heating various fiber lengths and to derive a correlation between fiber thickness or length and joule heating. From this investigation, it can be concluded that a voltage between 20 and 110 V was needed to achieve heating effect over lengths between 5 and 30 cm. Thermal properties revealed that a temperature T_{high} between 60 and 65 °C must be achieved to realize actuation in these fibers, which is related to the melting of oriented crystallites, whereas T_{low} could be ambient temperature or lower.

Finally, electrically triggered reversible actuation was investigated for coated fibers. Since the temperature ≈65 °C in composite fibers could not be achieved due to poor joule heating, actuation for these fibers was not investigated. For electrically triggered actuation, coated fibers were connected to electrodes and a certain voltage was applied to reach T_{high}. Results of a bending test are shown in Figure S7 (Supporting Information) for 5 cm cPEVA-CB2 fiber. The experiment consisted of five consecutive cycles, where T_{high} was achieved by switching ON the voltage source, while cooling to T_{low} (room temperature) was realized by switching the voltage source OFF. A voltage of 22 V was required to achieve 65 °C in this fiber. Here, a reversible actuation of 4–5% was observed, which was calculated from a change in height of fiber at T_{high} and T_{low}. Reversible actuation of coated fibers is primarily from contraction and expansion of the fiber core, where orientation of PE crystallites is achieved during the extrusion process (see WAXS results in Figure S8, Supporting Information). This orientation of crystallites is maintained in the fiber matrix after crosslinking. Oriented crystals melt during heating and result in entropic recovery and contraction of the fiber, while cooling results in recrystallization in the direction of orientation and consequently expansion of the fiber. Coating also contracts and expands with core fiber and was found quite stable for cPEVA-CB2. A clear advantage of electrical heating over conventional thermal heating can be observed regarding the time needed to heat the fiber. Evidently, the fiber can reach the required temperature in less than a minute, which in case of thermal actuation could be much longer depending on the temperature in an indirect heating method. Similarly, the cooling of the fiber by switching OFF the voltage source was quite fast. A detailed analysis of the time required for heating and cooling can be found in Figure S9 (Supporting Information).

Cyclic tests were performed for a detailed investigation of electrically triggered actuation of the coated fibers. For this purpose, electrodes were mounted on the clamps of a Zwick machine, while changes in temperature of specimen were monitored using an IR camera. Fiber length for these cyclic tests was 10 cm. Voltage (U) from 20 to 90 V were applied to heat the fiber via resistive/joule heating. Three temperatures (T_{high}) such as 50 °C or 65 °C (within the melting range) and 85 °C (above the melting range) were targeted. Six cycles were performed for each T_{high} achieved by applying voltage. Cooling was simply achieved by switching OFF the voltage source. A similar reversible change in length $\varepsilon'_{rev} = 5 \pm 1\%$ was observed for fibers with different coating thickness, while both conductivity and joule heating were not influenced during reversible actuation by expansion and contraction of fibers. No difference in reversible actuation was observed with change of T_{high}, however, a higher temperature led to further contraction of the specimen as can be seen in **Figure 4**A. Interestingly, reversible actuation was still observed when T_{high} was 85 °C, which is above the melting transition of PEVA. This can be attributed to the crosslinking of the core fiber after crystal orientation in the extrusion process. Post crosslinking of these at ambient temperature apparently allowed the crystalline domains within the fiber matrix to achieve permanent orientation,[22] which cannot be erased even after heating above melting transition. This allows the fiber to heat to higher temperatures without affecting reversible actuation.

Electrical actuation under stress was analyzed to investigate the adaptivity of these fibers to certain loads. However, the tests for the fibers with ≥10 µm coating thickness were not successful and resulted in breaking of coating under load and led to a non-conductive fiber. Therefore, the tests could only be performed for cPEVA-CB1 with a coating thickness of 10 ± 2 µm. For this purpose, weights on the fiber were varied as 10, 30, 100, 200, 300, and 400 g, whereas the fiber broke after three consecutive cycles at 400 g. The results revealed a decrease in

reversible change in length with an increase in applied load. An initial elongation related to higher weight occurs during the first heating cycle when the temperature increases to a range within the melting range of polymer. The reversible change in length is the actual change in length of the elongated fiber in subsequent heat–cool cycles by switching the voltage source ON and OFF. The actual change in length (ΔL) was calculated from analysis of picture series. The ΔL reduced from ≈6 to 0.5 mm with increase in the external load from 10 to 400 g, see Figure 4B. Furthermore, higher applied voltages were needed to achieve similar heating effect with increasing values of the external load. Changes in the applied voltage with varying loads are presented in Figure S10 (Supporting Information). This increase in voltage is due to an increase in fiber length and the breakdown in the conductive network due to stretching of the fiber under load.[13]

In order to investigate the effect of coating on reversible actuation, electrically triggered actuation of coated fibers was compared with thermal actuation of non-coated cPEVA fibers (as of core fiber). Cyclic thermomechanical tests were used for this analysis, which consisted of heating and cooling cycles without a conventional programming step. A similar T_{high} = 65 °C was selected for such tests, however, T_{low} = 10 °C below crystallization peak temperature was chosen. A reversible change in length $\varepsilon'_{rev} = 10 \pm 1\%$ was observed for cPEVA, which is almost double compared to electrical actuation of coated fibers. Coated fibers were investigated by similar cyclic thermomechanical test program as non-coated fibers with same parameters as can be observed in Figure S11 (Supporting Information). Coated fibers in these investigations showed low $\varepsilon'_{rev} = 5 \pm 1\%$ which was comparable to their electrical actuation, while fibers with different coating thickness showed similar actuation. Therefore, it can be concluded that lower ε'_{rev} of fibers is related to the coating, which hinders expansion and contraction of the fiber during reversible actuation.

Thermal actuation of composite fiber PEVA20CB10G was also analyzed. Since composite fibers were non-crosslinked, the actuation of these fibers was compared with non-crosslinked PEVA fibers. A lower T_{high} = 60 °C was used in these cyclic tests to observe reversible actuation. Figure S12 (Supporting Information) shows that these fibers elongate during first heating step to ≈100% followed by further elongation during cooling. The reversible effect in these fibers appeared to be under stress rather stress-free even with a small force. The observed reversible change in the strain ($\Delta\varepsilon$) was 20 ± 2% for PEVA fibers, however a creep effect was also observed within the five reversible cycles performed. A negligible $\Delta\varepsilon \approx 2 \pm 1\%$ was observed for PEVA20CB10G. Lower $\Delta\varepsilon$ of PEVA20CB10G could be related to poor crystallite orientation during the extrusion process.

3. Conclusion

In this study, we compared conductivity and resistive heating of composite and coated fibers and explored their suitability as electrically triggered actuators. A broad melting transition from 40 to 80 °C was observed for composite as well as coated conductive fibers and a temperature ≈60–65 °C within this melting range was considered suitable to trigger actuation. This temperature was to be achieved by joule heating, however conductivity of composite fibers was poor and the required temperature could not be realized. In contrast, higher conductivity of coated fibers allowed the required heating, where a voltage of 40 V was needed to achieve required actuation temperature for a fiber of 10 cm length, while 110 V for 30 cm long coated fibers. A reversible actuation of $\varepsilon'_{rev} = 5 \pm 1\%$ was observed for coated fibers which was lower than $\varepsilon'_{rev} = 10 \pm 1\%$ of thermally actuated non-coated cPEVA fibers. A decrease in ε'_{rev} for coated fibers is attributed to their coating, which hinders expansion and contraction of the core fiber during reversible actuation. The conductivity and the joule heating were not influenced during reversible actuation by expansion and contraction of fibers. Molecular orientation of the crystalline domains achieved during extrusion process was considered sufficient to enable actuation of the fibers. Moreover, reversible actuation performance of these fibers under stress was found to decrease with increase in applied load.

4. Experimental Section

Materials: Poly[ethylene-*co*-(vinyl acetate)] (PEVA) with a vinyl acetate content of 28 wt% (Elvax 260A, DuPont, triallyl isocyanurate (TAIC) (99%, Sigma-Aldrich, Steinheim, Germany), toluene (99.8% Sigma-Aldrich, Steinheim, Germany), carbon black (CB) (Super P conductive, 99+%, Alfa Aesar, ThermoFisher GmbH, Kandel, Germany), graphene nanoplatelets (Sigma-Aldrich, Steinheim, Germany) and carbon nanotubes (CNTs) (Sigma-Aldrich, Steinheim, Germany) were used as received.

Methods—Fiber Preparation: PEVA granulates 99 wt% and TAIC 1 wt% were manually mixed at first and afterward compounded in a twin-screw extruder (Euro Prism Lab, Thermo Fisher Scientific, Waltham, USA) with a temperature profile of 25, 80, 110, 110, 110, 110, and 100 °C (from feed to die) and at a screw-speed of 50 rpm. Then the blend granulates (PEVA+TAIC) were again extruded through a filament die to obtain fibers with a thickness of 0.4 ± 0.1 mm in a single screw extruder (Extrudex, Mühlacker, Germany) with an identical speed and temperature profile as used in compounding. These fibers were cross-linked by a gamma beam of 165 kGy. Non-crosslinked PEVA fibers were prepared by directly extruding PEVA in a single screw extruder (Extrudex, Mühlacker, Germany).

Methods—Conductive Fiber Coating: 1 g of PEVA was dissolved in 60 mL of toluene at 90 °C for 3 h. After cooling, 1, 2, 3, or 4 g of CB were added with additional 40 mL of toluene and the solution was kept stirring for overnight. Similarly, graphene and carbon nanotubes were also used to prepare coating solutions. Details of coating formulations can be found in Table S1, Supporting Information. The coating solution was applied to the crosslinked fibers via dip coating, where fibers were dipped four consecutive times in coating solution for 5 s.

Methods—Composite Fibers: Conductive fillers such as CB or graphene were first mixed with PEVA and 5 wt% ethanol. After evaporation of ethanol, the mixture was compounded in a twin-screw extruder (Euro Prism Lab, Thermo Fisher Scientific, Waltham, USA) with a temperature profile of 35, 80, 110, 115, 120, 100, and 80 °C (from feed to die) and a speed of 50 rpm. Afterward blend PEVA/filler granulates were extruded to obtain fibers in a single screw extruder (Extrudex, Mühlacker, Germany) with same speed and temperature as compounding. Details of composite fiber compositions are listed Table S1 (Supporting Information).

Conductivity of fibers was analyzed by Series 2410 SourceMeter (Keithley, Cleveland, Ohio, United States) with a source voltage range between 5 µV to 1100 V and a measure current range from 10 pA to 1.055 A. Crocodile shaped electrodes were used to connect the fibers

with the source meter, whereas the surface temperature was monitored by an infrared (IR) camera (Jenoptik AG, Jena, Germany).

SEM experiments of coated (PCL/carbon black) PEVA and cPEVA fibers were conducted at room temperature using a scanning electron microscope (Zeiss Supra 40VP, Zeiss, Oberkochen, Germany) operating at high vacuum with 1 to 3 kV, analyzed with an Everhart-Thornley detector (secondary electrons 2). For preparation of fibers' cross section, the filaments were first wetted with isopropanol, next frozen in liquid nitrogen and finally cracked with the help of a razor blade. The samples were coated with a 5 nm gold layer.

Methods—Differential Scanning Calorimetry (DSC): DSC measurements were performed on a calorimeter (Netzsch, Selb, Germany) DSC 204, with heating and cooling rates of 10 K min^{-1}. Weight % crystallinity was calculated with Equation (1).[23]

$$\chi_c = \frac{\Delta H_m}{\Delta H^{\circ}_{m/100}} \times 100 \quad (1)$$

where $\Delta H^{\circ}_{m/100}$ is the enthalpy of melting of 100% crystalline polymer, which is 287 J g^{-1} for polyethylene.[24]

Methods—Mechanical Properties: The mechanical properties of crosslinked fibers at ambient temperature were assessed by tensile tests on a Zwick Z2.5 (Zwick, Ulm, Germany) by elongation of samples until break. Five measurements were performed for each formulation to obtain elongation at break (ε_b) and Young's modulus (E). Samples had dimensions of 0.4 × 30 mm^2 (thickness, length). The pre-force was around 0.02 N and crosshead speed was 5 mm min^{-1}. Similarly, tensile tests at extended temperature (above melting temperature) were carried out on a Zwick Z1.0 (Zwick, Ulm, Germany) equipped with a thermochamber and temperature controller (Eurotherm Regler, Limburg, Germany).

Methods—Cyclic Tests for Electrical Actuation Investigations: The electrodes of the source meter were mounted with clamps of the Zwick machine, while temperature was continuously monitored by IR camera. A force of 50 mN was maintained on the specimen during reversible actuation. Heating to required actuation temperature (65 °C) was achieved by switching ON the voltage source while cooling to room temperatures was achieved by simply switching OFF the voltage source. A waiting time of 5 min was given at T_{high} and T_{low} to ensure complete actuation of the fibers. The related changes in length were analyzed by the following equations to estimate the reversible actuation.

Methods—Cyclic Thermomechanical Tests: Cyclic experiments (performed on Zwick Z1.0 with a thermochamber and temperature controller) were also performed to investigate thermal actuation. Such tests consisted of heating and cooling of the fiber under stress free conditions between T_{low} = 10 °C and T_{high} = 65 with 3 K min^{-1}. Quantification includes deformation fixation efficiency (Q_{ef}) as well as reversible change in length (ε'_{rev}) and were calculated from Equations (2) and (3)

$$\varepsilon'_{rev} = \frac{l_{T,low} - l_{T,high}}{l_{T,high}} \times 100 \quad (2)$$

$$Q_{ef} = \frac{\varepsilon_{T,high}}{\varepsilon_{prog}} \times 100 \quad (3)$$

where $l_{T,high}$ and $l_{T,low}$ are the lengths at T_{high} and T_{low} respectively in reversibility cycles, while $\varepsilon_{T,high}$ is the elongation at T_{high}.

Wide-angle X-ray Scattering (WAXS) measurements were performed using an X-ray diffraction system Bruker D8 Discover with a 2D Hi star-detector (105 µm pixel size) from Bruker AXS (Bruker, Karlsruhe, Germany). The X-ray generator produced Cu-K_α radiation (0.154 nm wavelength) and was operated at a voltage of 40 kV and a current of 40 mA on a copper anode. A graphite monochromator and a three-pinhole collimator with an opening of 0.8 mm defined the optical and geometrical properties of the beam. The distance between sample and detector was 150 mm, whereas the samples were illuminated for 2 min.

Methods—Statistics: The presented data in this study are average values with respective standard deviations (STD) based on experiments conducted at least in triplicate, unless stated otherwise. Morphological investigations were performed on 3–5 samples. Mechanical measurements were repeated at least five times and average values of elastic modulus and elongation at break were calculated along with STD. At least five fiber samples were analyzed for conductivity and joule heating analysis. The STD in reversible actuation were calculated from the changes in the different cycles within one cyclic test. The orientation at different cyclic temperatures were calculated from in-situ WAXS experiments with three repeating cycles.

Supporting Information

Supporting Information is available from the Wiley Online Library or from the author.

Acknowledgements

The authors thank Susanne Schwanz and Daniela Radzik for technical support. This work was financially supported by the Helmholtz Association through programme-oriented funding and has received funding from the European Union's Horizon 2020 research and innovation program under Grant Agreement No. 824074 (GrowBot).

Open access funding enabled and organized by Projekt DEAL.

Conflict of Interest

The authors declare no conflict of interest.

Keywords

artificial muscles, fiber actuators, resistive heating, shape-memory polymer actuators, soft robotics

Received: September 14, 2020
Revised: October 19, 2020
Published online: November 16, 2020

[1] L. Hines, K. Petersen, G. Z. Lum, M. Sitti, *Adv. Mater.* **2017**, *29*, 1603483.
[2] A. Lendlein, O. E. C. Gould, *Nat. Rev. Mater.* **2019**, *4*, 116.
[3] J. Shintake, V. Cacucciolo, D. Floreano, H. Shea, *Adv. Mater.* **2018**, *30*, 1707035.
[4] M. Behl, K. Kratz, U. Noechel, T. Sauter, A. Lendlein, *Proc. Natl. Acad. Sci. USA* **2013**, *110*, 12555.
[5] G. V. Stoychev, L. Ionov, *ACS Appl. Mater. Interfaces* **2016**, *8*, 24281.
[6] J. K. Yuan, P. Poulin, *Science* **2014**, *343*, 845.
[7] J. Fan, G. Li, *RSC Adv.* **2017**, *7*, 1127.
[8] C. S. Haines, M. D. Lima, N. Li, G. M. Spinks, J. Foroughi, J. D. W. Madden, S. H. Kim, S. L. Fang, M. J. de Andrade, F. Goktepe, O. Goktepe, S. M. Mirvakili, S. Naficy, X. Lepro, J. Y. Oh, M. E. Kozlov, S. J. Kim, X. R. Xu, B. J. Swedlove, G. G. Wallace, R. H. Baughman, *Science* **2014**, *343*, 868.
[9] J. Foroughi, G. M. Spinks, G. G. Wallace, J. Oh, M. E. Kozlov, S. L. Fang, T. Mirfakhrai, J. D. W. Madden, M. K. Shin, S. J. Kim, R. H. Baughman, *Science* **2011**, *334*, 494.
[10] A. Lendlein, *Sci. Robot.* **2018**, *3*, eaat9090.

[11] J. K. Yuan, W. Neri, C. Zakri, P. Merzeau, K. Kratz, A. Lendlein, P. Poulin, *Science* **2019**, *365*, 155.
[12] H. Kim, S. Lee, H. Kim, *Sci. Rep.* **2019**, *9*, 1511.
[13] A. T. Chien, S. Cho, Y. Joshi, S. Kumar, *Polymer* **2014**, *55*, 6896.
[14] L. S. Wu, L. Wang, Z. Guo, J. C. Luo, H. G. Xue, J. F. Gao, *ACS Appl. Mater. Interfaces* **2019**, *11*, 34338.
[15] J. Park, J. W. Yoo, H. W. Seo, Y. Lee, J. Suhr, H. Moon, J. C. Koo, H. R. Choi, R. Hunt, K. J. Kim, S. H. Kim, J. D. Nam, *Smart Mater. Struct.* **2017**, *26*, 035048.
[16] E. Enriquez, J. de Frutos, J. F. Fernandez, M. A. de la, Rubia, *Compos. Sci. Technol.* **2014**, *93*, 9.
[17] H. S. Wang, J. Cho, D. S. Song, J. H. Jang, J. Y. Jho, J. H. Park, *ACS Appl. Mater. Interfaces* **2017**, *9*, 21998.
[18] H. Meng, G. Q. Li, *Polymer* **2013**, *54*, 2199.
[19] H. H. Le, I. Kolesov, Z. Ali, M. Uthardt, O. Osazuwa, S. Ilisch, H. J. Radusch, *J. Mater. Sci.* **2010**, *45*, 5851.
[20] M. Farhan, T. Rudolph, K. Kratz, A. Lendlein, *MRS Adv.* **2018**, *3*, 3861.
[21] J. S. Leng, H. B. Lv, Y. J. Liu, S. Y. Du, *Appl. Phys. Lett.* **2007**, *91*, 144105.
[22] Y. Meng, J. S. Jiang, M. Anthamatten, *ACS Macro Lett.* **2015**, *4*, 115.
[23] A. Ujhelyiova, A. Marcincin, J. Legen, *Fibres Text. East. Eur.* **2005**, *13*, 129.
[24] C. P. Fonseca, F. Cavalcante, F. A. Amaral, C. A. Z. Souza, S. Neves, *Int. J. Electrochem. Sci.* **2007**, *2*, 52.